



OPTIMIZING CORROSION INHIBITION OF COPPER IN SULFURIC ACID USING MAGNESIUM-DOPED MESOPOROUS MANGANESE SILICATE: EXPERIMENTAL AND RESPONSE SURFACE METHODOLOGY ANALYSIS

Chahrazed DAOUDI,^{a*} Fatiha HAMIDI,^a Abbas BENCHADLI,^b Tarik ATTAR,^{b,c} Karima SAIDI-BENDAHOU^a and Chewki Ziani CHERIF^a

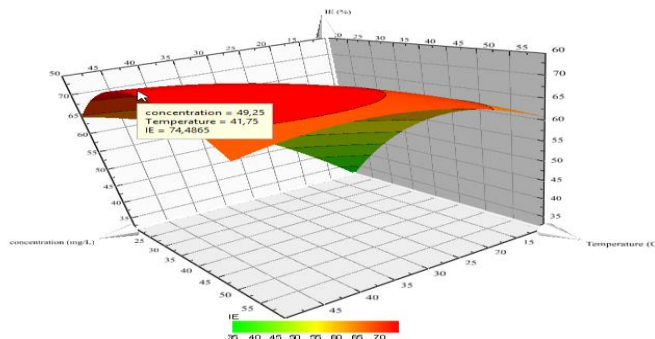
^aLaboratory of Catalysis and Organic Synthesis LCSCO, Department of Chemistry, University of Tlemcen, BP 119, Tlemcen, Algeria

^bToxicoMed laboratory, University of Tlemcen, BP119, Tlemcen, Algeria

^cTlemcen Higher School of Applied Sciences, ESSA-Tlemcen, BP 165 RP Bel Horizon, Tlemcen, Algeria

Received November 3, 2024

Corrosion, though inevitable, can be effectively mitigated to extend material lifespan. This study investigates the efficacy of mesoporous manganese silicate doped with magnesium as a corrosion inhibitor for copper in sulfuric acid. The inhibitor's performance was evaluated under varying conditions of concentration, temperature, and exposure duration, revealing a positive correlation between these variables and inhibition efficiency. The activation energy for corrosion in the inhibited system was significantly higher than in the non-inhibited system, indicating enhanced protection. Adsorption studies confirmed that the inhibitor molecules adhered spontaneously to the copper surface, following Langmuir, Freundlich, and Temkin isotherms, suggesting a mixed adsorption mechanism. Scanning electron microscopy (SEM) analysis corroborated the formation of a protective organic layer on the copper surface. Response surface methodology (RSM) coupled with regression statistical analysis and probabilistic assessment was employed to optimize and validate the experimental data. The quadratic models for inhibition efficiency (IE) demonstrated exceptional accuracy, with a coefficient of multiple regressions (R^2) of 0.996 and an adjusted R^2 of 0.992, indicating a strong fit between experimental and predicted values. The model's predictive capability was further validated by a Q^2 value of 0.961 and a reproducibility value of 0.999, nearly equivalent to unity. The inhibitor exhibited remarkable inhibitory power, exceeding 84% in both experimental and predictive calculations. These findings highlight the potential of magnesium-doped mesoporous manganese silicate as a highly effective and reproducible corrosion inhibitor for copper in acidic environments.



INTRODUCTION

Copper is a vital metal renowned for its exceptional properties, particularly its outstanding electrical and thermal conductivity, making it the

material of choice for electrical wiring, electronic components, and heating and cooling systems.^{1,2} In addition to its conductive properties, copper exhibits remarkable resistance to corrosion.³ When exposed to air and water, it forms a protective layer known as

* Corresponding author: chahrazedddk@gmail.com

patina, which significantly slows down degradation and extends the lifespan of copper-based products.⁴ This characteristic makes copper highly valuable in applications such as plumbing, roofing, and architectural structures.⁵ Historically, copper has played a pivotal role in the advancement of human civilization, notably during the Bronze Age. In modern times, its unique properties continue to meet the demands of advanced technologies while contributing to sustainability due to its recyclability and abundant availability.⁶ To further enhance copper's resistance to corrosion, chemical inhibitors – both inorganic and organic – can be employed to delay or prevent corrosive processes.⁷

Mesoporous materials have emerged as highly effective reservoirs for corrosion inhibitors due to their unique porous structure and large surface area, with pore sizes typically ranging from 2 to 50 nm.^{8,9} Composed primarily of silicates or aluminosilicates, these materials provide durable corrosion protection by selectively adsorbing corrosive agents and releasing them in a controlled manner.¹⁰ Recent studies have demonstrated growing interest in the use of mesoporous materials as corrosion inhibitors, including variants such as Cu/SBA15, Ni/SBA15, TiO₂,¹¹ CeO₂,¹² GO/ZnO,¹³ SiO₂,¹⁴ and Ni-CO-MSNs.¹⁵

Design of Experiments (DOE) is a systematic methodology used to plan, design, and analyze experiments.¹⁶ It enables researchers to understand the relationships between various process factors and their outcomes.¹⁷ By controlling independent variables (factors) and evaluating their effects on dependent variables (responses), DOE enhances experimental efficiency by optimizing processes with minimal trials while improving accuracy through structured analysis.^{18,19} This approach also facilitates the identification of interactions between factors and their combined effects on responses. The application of experimental design methods yields more precise results for key metrics, such as inhibition efficiency (IE), and provides insights into the interactions among studied parameters.²⁰ Response Surface Methodology (RSM), a subset of DOE, is particularly useful for modeling and optimizing responses influenced by multiple variables.^{21,22} It is widely employed to identify optimal process conditions and understand complex interactions between variables.²³ In this study, we focus on investigating a novel corrosion inhibitor formulation in a sulfuric acid medium, utilizing mesoporous manganese silicate doped with magnesium (1.5% Mg-MMnS-n, where n = Si/Mn = 20) of the SBA-15 type.^{24,25} The research aims to evaluate the corrosion inhibition performance of

this material in a 0.5M H₂SO₄ solution using weight loss measurements, DOE, and RSM. Specifically, the study examines the interactive effects of inhibitor concentration, operating temperature, and immersion duration on inhibition efficiency. Additionally, various adsorption isotherm models and thermodynamic parameters related to inhibitor adsorption on the copper surface are estimated and discussed. Scanning Electron Microscopy (SEM) is employed to further validate the adsorption of the inhibitor on the copper surface, providing visual evidence of its protective effects.

EXPERIMENTAL

1. Material preparation

Copper specimens were utilized in weight loss experiments to study corrosion inhibition. Before testing, the copper samples were polished with a series of emery papers ranging from 600 to 1200 grit, followed by thorough washing with water and acetone (99%, Sigma-Aldrich, Germany). A 0.5 M sulfuric acid solution was prepared by diluting concentrated H₂SO₄ (98%, Merck, Germany) with distilled water. The inhibitor concentration in the acidic solution was adjusted to vary between 10 and 50 mg/L.

2. Weight loss measurements

The weight-loss method measures the corrosion rate by determining the mass loss of a metal sample over a specific period of exposure to a corrosive environment. This technique provides more accurate results for uniform corrosion than electrochemical methods because it mirrors actual experimental conditions.²⁶ Weight loss measurements were carried out according to the protocols described in our previous studies.^{27,28} Each measurement was performed three times, and the average weight losses were recorded and reported.

The following equations were used to calculate the corrosion rate without the inhibitor (CR), with the inhibitor (CR_{inh}), and the inhibition efficiency (IE):

$$CR = \Delta w / (S \times t) \quad (1)$$

$$IE(\%) = 100 \times (CR - CR_{inh}) / CR \quad (2)$$

where Δw refers to the weight loss in milligrams (mg), S stands for the sample area in square centimeters (cm²), and t symbolizes the immersion time in hours (h).

3. Adsorption Isotherm and Thermodynamic Parameter Determination

Adsorption isotherms are graphical representations that illustrate the relationship between the amount of adsorbate retained on an adsorbent surface and the concentration of the adsorbate in the surrounding environment at a constant temperature. In the study of organic substance absorption within the body, these isotherms offer valuable insights into how these substances interact with surfaces.

To determine the adsorption mode of plant-based inhibitors, various authors commonly employ Langmuir, Temkin, Freundlich, Frumkin, and El-Awady isotherms. These isotherms describe the correlation between the recovery rate and inhibitor concentration as follows:

Langmuir adsorption isotherm is represented by Eq. (3):²⁸

$$C/\theta = 1/K_{ads} + C \quad (3)$$

Temkin adsorption isotherm model:²⁹

$$\theta = \ln C + K_{ads} \quad (4)$$

Freundlich adsorption isotherm:³⁰

$$\log(\theta) = n \log C + \log K_{ads} \quad (5)$$

Frumkin adsorption isotherm model:³¹

$$\log[C(\theta/1-\theta)] = 2\alpha\theta + 2.303 \log K_{ads} \quad (6)$$

El-Awady adsorption isotherm is formulated as follows:³²

$$\log(\theta/1-\theta) = y \log(C) + y \log K_{ads} \quad (7)$$

Flory-Huggins adsorption isotherm is expressed by Eq. (8):²⁹

$$\log(\theta/C) = b \log(1-\theta) + \log K_{ads} \quad (8)$$

In this context, C denotes the inhibitor concentration, K_{ads} represents the adsorption-desorption equilibrium constant, θ signifies the surface coverage by the inhibitor, n is the Freundlich exponent, a positive constant, α characterizes the lateral interactions within the adsorbed layer, b refers to the size parameter, indicating the displacement of adsorbed water molecules by a single inhibitor molecule, and y represents the number of inhibitor molecules that occupy a single active site.

4. Determination of Thermodynamic Activation Parameters

The activation energy of a reaction, both with and without an inhibitor, can be determined by rearranging the Arrhenius equation. The relationship between the activation energy and the corrosion rate is expressed as follows:

$$\ln(\text{CR}) = -E_a/RT + \ln A \quad (9)$$

where CR is the corrosion rate, E_a is the activation energy, R is the gas constant, T is the absolute temperature, and A is the Arrhenius pre-exponential factor. According to this equation, the activation energy is represented by the slope of the Arrhenius plot, which is a plot of $\ln(\text{CR})$ versus $1/T$.

The enthalpy (ΔH_a) and entropy (ΔS_a) of activation can be determined using the transition state theory, which is an alternative to the Arrhenius equation:

$$\ln(\text{CR}/T) = -\Delta H_a/RT + \ln(R/Nh) + (\Delta S_a/R) \quad (10)$$

where h is Planck's constant, and N is the Avogadro's number. Enthalpy of activation

(ΔH_a) is measured as the slope of a straight line by plotting $\ln(\text{CR}/T)$ versus $1/T$ in equation (10), and the entropy of activation (ΔS_a) can be calculated from its intercept.

5. Design of experiments study

The experiments were designed and statistically analyzed using MODDE Version 9.1 software. The main objective was to develop a precise analytical model to evaluate the impact of various variables on the response and determine the optimal conditions. To achieve this, response surface methodology (RSM) was employed to estimate the model coefficients and optimize the experimental design. The parameters studied in sulfuric acid included inhibitor concentration (X1), temperature (X2), and immersion time (X3), each at three distinct levels. Details of the independent parameters and their levels are provided in Table 1.

Table 1

Optimization of inhibition efficiency of an Mg-MMnS on copper in acid medium: weight loss and RSM approach

Symbol	Independent variable	Units	Levels		
			-1	0	+1
X1	Concentration	mg/L	10	30	50
X2	Temperature	°C	20	40	60
X3	Time	h	0.5	1	1.5

RESULTS AND DISCUSSION

1. Adsorption Isotherm and Determination of Adsorption Thermodynamic Parameters

Adsorption isotherms graphically represent the relationship between the amount of adsorbate retained on an adsorbent surface and the concentration of the adsorbate in the surrounding environment. These studies are crucial for understanding how organic substances interact with

surfaces. Various authors use the Langmuir, Temkin, Freundlich, Frumkin, and El-Awady isotherms to determine the adsorption mode of inhibitors.³⁰

The results presented in Table 2 indicate that the Langmuir, Freundlich and Temkin isotherms are the most suitable for describing our case study. This selection is justified by the correlation coefficient R^2 being close to 1 for the Mg-MMnS inhibitor. Therefore, these methods were validated for evaluating the adsorption parameters.

Table 2

R^2 values for the various adsorption isotherms considered

T (K)	R^2					
	Langmuir	Temkin	Freundlich	Flory-Huggins	El-Awady	Frumkin
293	0.991	0.991	0.999	0.963	0.991	0.991
303	0.978	0.970	0.993	0.949	0.970	0.975
313	0.987	0.975	0.984	0.969	0.975	0.955
323	0.994	0.981	0.985	0.971	0.981	0.959
333	0.996	0.983	0.979	0.979	0.982	0.952

The evaluation of the free energy of inhibitor adsorption on the copper surface involves employing the following equation:³¹

$$\Delta G_{\text{ads}} = -RT \ln(1000 K_{\text{ads}}) \quad (11)$$

where, R represents the gas constant (J/mol K), and T denotes the absolute temperature (K). The value of

1000 corresponds to the concentration of water in the solution (mg/L). K_{ads} signifies the adsorption equilibrium constant, reflecting the strength of interaction between the inhibitor and the metal surface. The equilibrium constant (K_{ads}) for the adsorption process was determined through graphical analysis of the relevant adsorption isotherm.

Table 3

Thermodynamic parameters for the adsorption of Mg-MMnS ($n = 20$) on copper surface in sulfuric acid at different temperatures

T (K)	K_{ads} (L/g)	ΔG_{ads} (kJ/mol)	ΔH_{ads} (kJ/mol)	ΔS_{ads} (J/mol K)
293	474.48	-31.82		
303	574.17	-33.38		
313	705.75	-35.03	17.13	-166.88
323	919.35	-36.85		
333	1074.88	-38.43		

The thermodynamic parameters of inhibitor adsorption offer crucial insights into the mechanism of corrosion inhibition. An

exothermic adsorption enthalpy can indicate either chemisorption, physisorption, or a combination of both. Conversely, an endothermic

adsorption enthalpy typically suggests chemisorption. A negative change in entropy during adsorption suggests reduced degradation of the metal surface, whereas a positive change indicates increased system disorder. Negative free energy values indicate a spontaneous adsorption process. In this study, as shown in the table above, the adsorption equilibrium constant rises with increasing temperature, indicating that higher temperatures enhance the adsorption of the inhibitor on the copper surface rather than promoting desorption.³²

The ΔG_{ads} values range from -31.82 to -38.43 kJ/mol at temperatures between 293 and 333 K, suggesting a mixed adsorption mechanism ($\Delta G_{\text{ads}} > -20$ kJ/mol implies physisorption, while values ≤ -40 kJ/mol indicate chemisorption).³³ The positive values of ΔH_{ads} confirm that the adsorption of inhibitors is an endothermic and chemical process.³⁴ A negative change in entropy further signifies a reduction in metal surface degradation.³⁵ The calculated enthalpy and free energy values indicate a combination of physical and chemical interactions between the inhibitor and the metal surface, with a tendency towards chemisorption.

2. Activation energy calculations

The activation energy values obtained in this study are consistent with data reported in the literature. It is evident that the activation energy (E_a) values are lower in the presence of the inhibitor compared to its absence,³⁶ which suggests chemical adsorption of the inhibitor onto the metal surface. Positive values of the free energy of activation ($\Delta G_a > 0$) indicate that the corrosion reaction is non-spontaneous and becomes more pronounced with increasing inhibitor concentration. This suggests that the corrosion reaction requires an input of energy to proceed. Furthermore, the observed increase in ΔG_a values in the presence of the inhibitor compared to its absence suggests that the inhibitor's introduction enhances the thermodynamic barrier against the corrosion reaction. Positive values of the enthalpy ΔH_a reflect the endothermic nature of copper part dissolution and mean that copper dissolution is difficult.³⁷ Comparing the ΔS_a values reveals that the entropy of activation decreases in the presence of the studied inhibitor compared to the free acid. The reduced ΔS_a value further supports the slowed metal dissolution when inhibitor is present.³⁸

Table 3

Activation parameters for copper dissolution in 0.5M H₂SO₄ in the absence and presence of various concentrations of 1.5% Mg-MMnS-n, (n = 20)

$C_{\text{inh}}(\text{mg/L})$	R^2	E_a (kJ/mol)	R^2	ΔH_a (kJ/mol)	ΔS_a (J/mol.K)	ΔG_a (kJ/mol)
0	0.994	42.39	0.993	39.79	-186.68	56.60
10	0.990	33.13	0.991	30.13	-223.56	65.53
20	0.983	29.42	0.980	24.48	-243.54	73.81
30	0.973	19.78	0.990	16.88	-270.14	84.57
40	0.977	14.98	0.985	12.31	-287.51	92.87
50	0.996	12.10	0.994	9.49	-298.50	99.41

3. Design of experiments study

3.1. Optimization of inhibition efficiency using RSM

A total of 17 experimental trials were performed to assess the inhibition efficiency (IE) using three

independent variables: inhibitor concentration (X_1), temperature (X_2), and immersion time (X_3). The experimental design is outlined in Table 4. The resulting equation, expressed in terms of actual factors, is as follows:

$$\text{IE}(\%) = 69.513 + 15.33x_1 + 16.054x_2 + 3.607x_3 - 3.724x_1^2 - 2.239x_2^2 - 13.394x_3^2 + 2.541x_1x_2 + 0.038x_1x_3 - 1.578x_2x_3$$

Table 4

Responses of experimental design for inhibition process of copper in the presence of 1.5% Mg-MMnS (n = 20) drug in 0.5 mol/L of H₂SO₄

Run order		Facteurs						IE (%)
EXP N°		X1: Concentration		X2: Temperature		X3: Time		
		Coded	Real	Coded	Real	Coded	Real	
1	11	-1	10	-1	20	-1	0.5	17.83
2	4	+1	50	-1	20	-1	0.5	41.12
3	3	-1	10	+1	60	-1	0.5	46.33
4	6	+1	50	+1	60	-1	0.5	83.04
5	7	-1	10	-1	20	+1	1.5	25.47
6	9	+1	50	-1	20	+1	1.5	52.17
7	2	-1	10	+1	60	+1	1.5	50.91
8	17	+1	50	+1	60	+1	1.5	84.52
9	1	-1	10	0	40	0	1	49.18
10	12	+1	50	0	40	0	1	82.26
11	15	0	30	-1	20	0	1	51.04
12	10	0	30	+1	60	0	1	83.37
13	8	0	30	0	40	-1	0.5	50.39
14	5	0	30	0	40	1	1.5	61.71
15	16	0	30	0	40	0	1	68.94
16	13	0	30	0	40	0	1	69.73
17	14	0	30	0	40	0	1	70.15

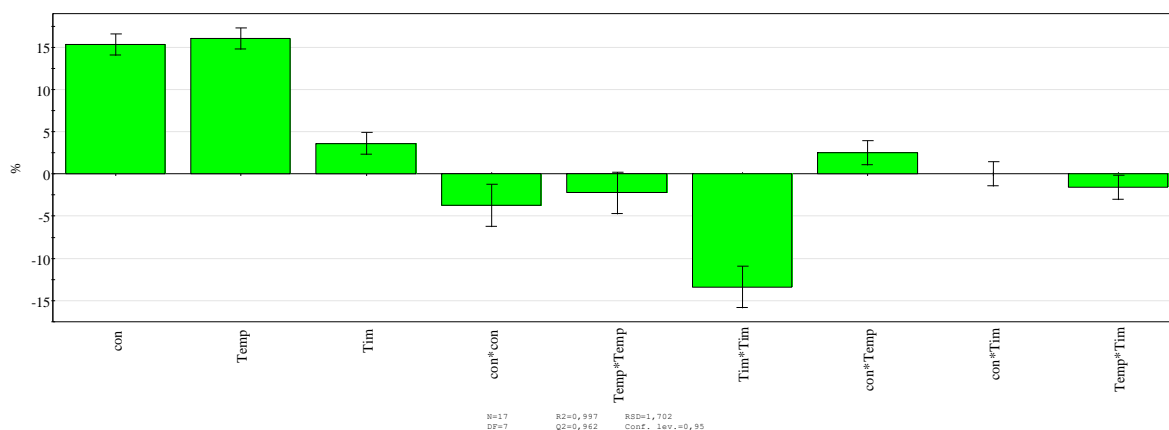


Fig. 1 – The effects of factors and interactions.

The histograms in Fig. 1 illustrate the effects of various factors and their interactions on the inhibition efficiency (IE) of 1.5% Mg-MMnS (n = 20).

All parameters temperature, concentration, and immersion time significantly influence IE%, as indicated by their respective absolute values. In the model, coefficients with positive values

demonstrate a synergistic effect, while those with negative values indicate an antagonistic effect.³⁵ Specifically, the interaction term Con*Tem contributes positively to the model, whereas Con², Temp², Tim², and Temp*Tim have a negative influence on its formulation. Additionally, the interaction term Con*Tim has no significant effect.

Table 5

Coefficients of factors, interactions, and probability values of approximate polynomials for response variables are displayed in the experimental design.

	R ²	R ² Adj.	Q ²	RSD	Model Validity	Reproducibility
IE	0.996	0.992	0.961	1.702	0.398	0.999

The Q² value measures the model's effectiveness for future predictions, and Q² should be greater than

0.1 for a significant model and greater than 0.5 for a good model.³⁹ In addition, for a good model (Q² >

0.9).⁴⁰ the validity of the model may still be low due to high test sensitivity or very good repetitions. According to Table 5, the Q^2 obtained for IE is greater than 0.9 ($Q^2 = 0.961$), indicating a good model in this study. The IE indicates high dependence and good correlation between observed and predicted response values. Figure 2 clearly

shows that the data points on the graph are distributed reasonably close to the straight line as the R^2 value of 0.996, The IE (%) indicates that there is a good relationship between experimental and predicted response values, and the t-model equations can be reliably useful for sampling data within the experimental parameter range.⁴¹

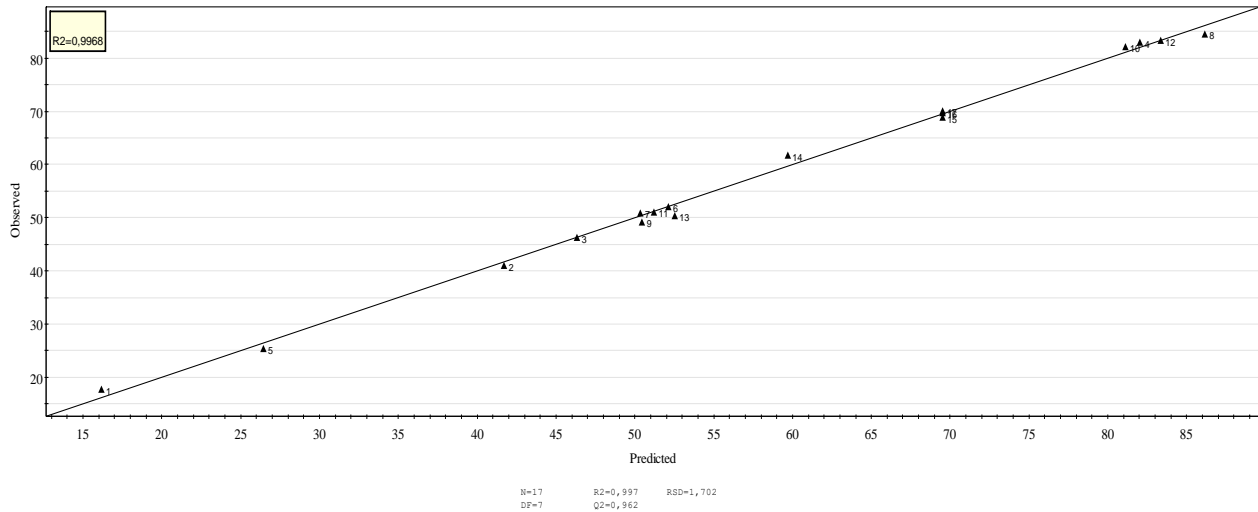


Fig. 2 – Diagnostic representation of predicted versus observed inhibition efficiency.

3.2. Main Effects

Figure 3 shows the impact of each parameter examined. We noticed that as the inhibitor concentration increased, the inhibitor efficacy (IE%) also increased.

Under static conditions, the highest inhibition

efficiency (IE) is achieved when copper is immersed in a 50 mg/L sulfuric acid solution for 1 hour at a temperature of 45°C. Conversely, a lower IE% is observed when copper is exposed to a 10 mg/L sulfuric acid solution, immersed for 30 minutes, and maintained at 20°C.

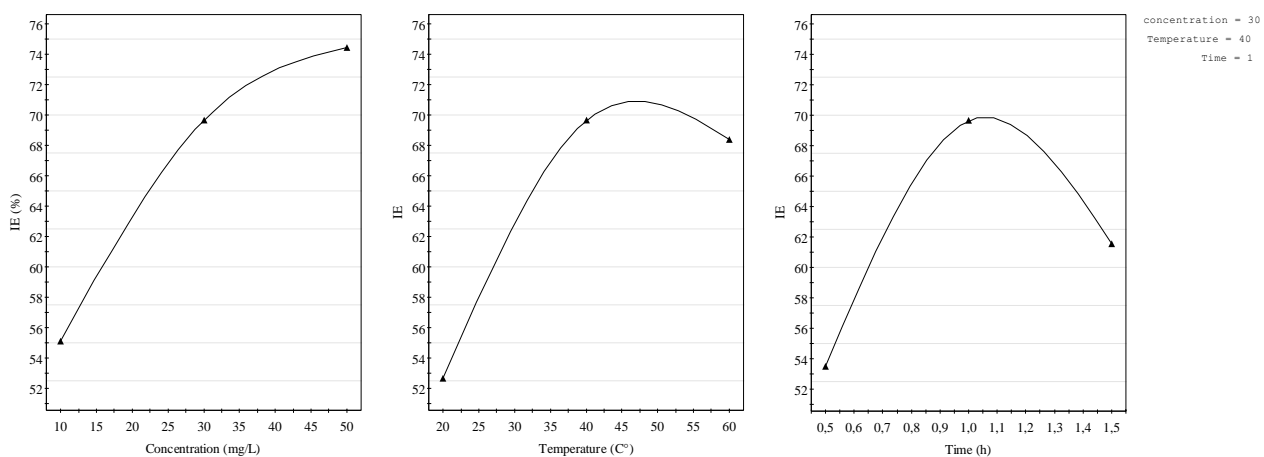


Fig. 3 – Main graph plot for inhibition efficiency.

3.3. Response Surface and Contour Plots

To check the effects of the three parameters on the IE (%) and observe the optimum zone

for the two responses, the best way is to plot response surfaces and 4D contours (Figs. 4 and 5).

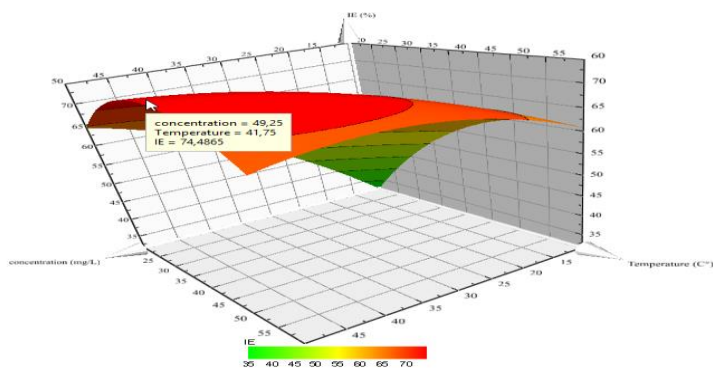


Fig. 4 – Surface plot of inhibition efficiency at optimum conditions.

The inhibition efficiency (IE) improves significantly as the temperature increases for a given concentration of the inhibitor. This enhancement in IE (%) is primarily due to the adsorption of Mg-MMnS inhibitor molecules onto the metal surface, which facilitates a chemical adsorption process. As the inhibitor concentration rises from its minimum to

maximum level, the IE (%) further increases with increasing temperature. For any quantity of Mg-MMnS ($n = 20$) in the system, the IE improves with immersion time, reaching optimal performance within 1 hour. The highest IE is achieved at a temperature of 41.75°C and the maximum concentration of Mg-MMnS- n ($n = 20$), as demonstrated in Fig. 5.

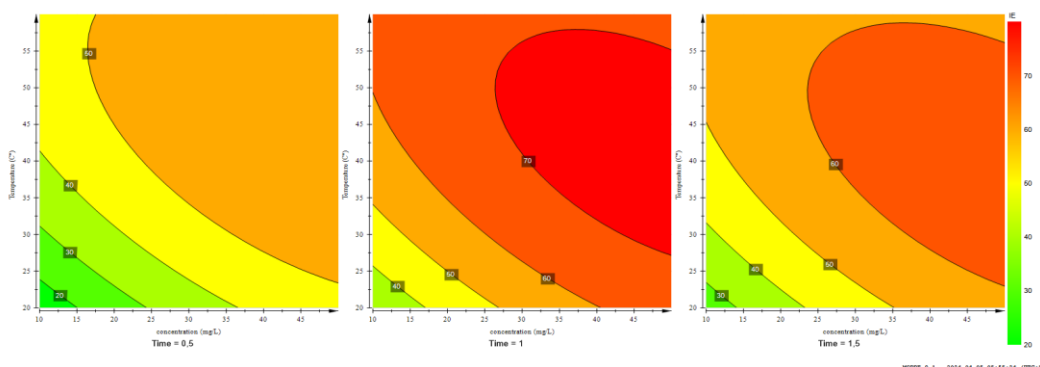


Fig. 5 – 4D Contour plots of effects of temperature and concentration on inhibition efficiency.

4. Scanning Electron Microscopy

To evaluate the effectiveness of the inhibitor in protecting copper against corrosion in a sulfuric acid environment, SEM imaging was conducted. Initially, the copper sample displayed a smooth and uniform surface, as depicted in Fig. 6a. However, after exposure to a $0.5\text{ M H}_2\text{SO}_4$ solution, significant pitting corrosion was observed (Fig. 6b). The application of

the inhibitor resulted in a notable reduction in the corrosion rate, as illustrated in Fig. 6c. Visual analysis revealed a substantial decrease in surface cracks and pitting compared to the untreated sample in Fig. 6b. This improvement is attributed to the adsorption of 1.5% Mg-MMnS compounds onto the copper surface. Furthermore, the treated sample exhibited a more uniform surface morphology in the acidic medium, indicating enhanced corrosion protection.⁴²

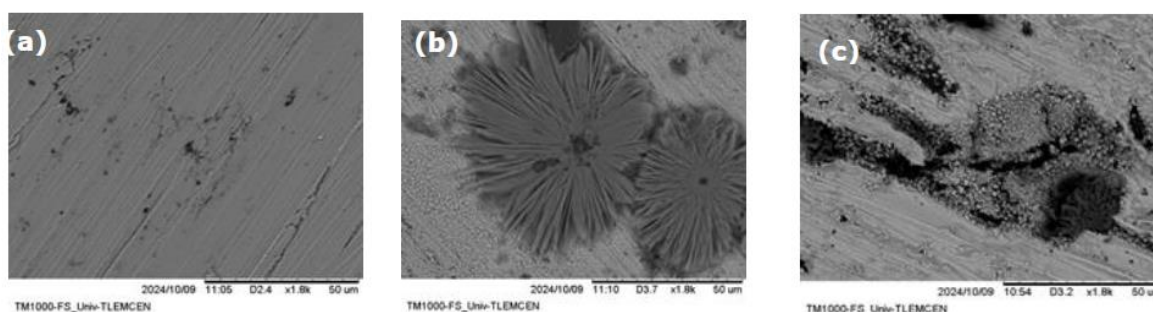


Fig. 6 – SEM images of copper samples exposed to corrosion in a $0.5\text{ M H}_2\text{SO}_4$ solution: a) before immersion (polished); b) without 1.5% Mg-MMnS; c) with 1.5% Mg-MMnS.

CONCLUSION

This study investigated the inhibition of copper corrosion in a sulfuric acid medium using a mesoporous material, with weight loss measurements conducted under varying conditions of concentration, immersion time, and temperature. The results demonstrate that magnesium-doped mesoporous manganese silicate (1.5%Mg-MMnS) is an effective corrosion inhibitor in sulfuric acid, exhibiting high inhibition efficiency. However, the inhibitor's performance decreases with increasing temperature, leading to an accelerated corrosion rate in the acidic environment. The adsorption of 1.5%Mg-MMnS onto the copper surface, supported by adsorption enthalpy values, confirms the endothermic nature of the process. The calculated free energy values indicate that the adsorption is spontaneous and involves both physical and chemical interactions, with a predominance of chemisorption. Scanning electron microscopy (SEM) images further validate the formation of a protective layer on the copper surface, highlighting the inhibitor's effectiveness. Numerical optimization of the corrosion inhibition process for 1.5%Mg-MMnS revealed that the optimal conditions for achieving maximum inhibition efficiency (IE) of 84.54% include a temperature of 60°C, an inhibitor concentration of 50 mg/L, and an immersion time of 1 hour. Using response surface methodology (RSM) combined with analysis of variance (ANOVA), robust predictive models for IE were developed. The accuracy and reliability of these models were confirmed through R² statistics, adequate precision values, and diagnostic plots.

Acknowledgements. The research team gratefully acknowledges the financial support provided by the Ministry of Higher Education and Scientific Research of the Algerian Government and the Higher School of Applied Sciences. The authors also extend their sincere appreciation to the University of Tlemcen for their invaluable technical assistance throughout this study.

REFERENCES

- Alfalah MGK, Elid A, Ali AAA, Kamberli E, Nazlı B, Koyun S *et al.*, Improvement of corrosion resistance for brass in 3.5% NaCl media by using 4-fluorophenyl-2, 5-dithiohydrazodicarbonamide, *Journal of the Turkish Chemical Society Section A: Chemistry*, **2023**, *10*(4), 869–876. <DOI>.
- Karakoç V, Erçağ E, New Generation Nanoadsorbents and Conventional Techniques for Arsenic Removal from Waters, *Journal of the Turkish Chemical Society Section A: Chemistry*, **2024**, *11*(2), 845–868. <DOI>.
- Attar T, Benchadlı A, Studying the Effectiveness of an Expired Betamethasone Drug in Sulfuric Acid Solutions to Examine the Corrosive Behavior of Copper Using Weight Loss and Experimental Design, *Journal of the Turkish Chemical Society Section A: Chemistry*, **2024**, *11*(1), 291–302. <DOI>.
- Ugi B, DFT and Electrochemical Study of Novel Green Corrosion Inhibitor (Pyrantrin) for 1100-H14 Aluminum Corrosion Remediation in 1 M H₂SO₄ Acidic Environment, *Journal of the Turkish Chemical Society Section A: Chemistry*, **2024**, *11*(1), 253–560. <DOI>.
- Salwathura K, Shabani F, Evaluating Environmental Impacts: Embodied Carbon Assessment of Ventilation, Electrical, and Plumbing Systems in Swedish School Architecture, 2024, <DOI>.
- Boccaccini F, Riccucci C, Messina E, Pascucci M, Bosi F, Aldega L *et al.*, Early Stages of Metal Corrosion in Coastal Archaeological Sites, Effects of Chemical Composition in Silver and Copper Alloys, *Materials*, **2024**, *17*(2), 442. <DOI>.
- Zhang H, Zhang X, Bian H, Zhang L, Chen Y, Yang Y *et al.*, Benzotriazole loaded CeO₂ nano-containers towards superior anti-corrosive silane coating for protection of copper, *Colloids and Surfaces A: Physicochemical and Engineering Aspects*, **2024**, 682, 132844. <DOI>.
- Gençer A, Karataş BU, Topel Ö, Kiraz N, Synthesis and characterization of surface-modified magnetic mesoporous silicate materials for phosphate adsorption, *Turkish Journal of Chemistry*, **2024**, *48*(1), 50–64. <DOI>.
- Gür GG, Toprak B, Optimized intermediate layer formation and electroless plating methods to obtain supported dense Pd surfaces, *Turkish Journal of Chemistry*, **2024**, *48*(1), 195–209. <DOI>.
- Arli OT, Gök Y, Gök HZ, pH responsive curcumin released from urea-amine group functionalized mesoporous organosilica nanoparticles, *Turkish Journal of Chemistry*, **2023**, *47*(6), 1518–1528. <DOI>.
- Badene R. Synthèse de matériaux mesoporeux pour une adsorption efficace de CO₂ du gaz naturel, 2023, <DOI>.
- Venkatachalam D, Govindaraj Y, Prabhakar M, Ganapathi A, Sakairi M, Rohwerder M *et al.*, Smart release of turmeric as a potential corrosion inhibitor from a pH-responsive polymer encapsulated highly ordered mesoporous silica containers, *Surfaces and Interfaces*, **2024**, *45*, 103883. <DOI>.
- Ramazanoğlu D, Composite Materials in Biomimetic Nanohybrid Structures for Analytical Chemistry, *Surface Chemistry, and Corrosion*, <DOI>.
- Yin Y, Zhao H, Prabhakar M, Rohwerder M, Organic composite coatings containing mesoporous silica particles: Degradation of the SiO₂ leading to self-healing of the delaminated interface, *Corrosion Science*, **2022**, *200*, 110252. <DOI>.
- Bai S, Liu X, Xu L, Xuan J, Liu Y, Shao Y *et al.*, Enhancement of corrosion resistance and lubricating performance of electrodeposited Ni-Co coating composited with mesoporous silica nanoparticles and silicone oil impregnation, *Materials Chemistry and Physics*, **2022**, *282*, 125929. <DOI>.
- Rampado R, Peer D, Design of experiments in the optimization of nanoparticle-based drug delivery systems, *Journal of Controlled Release*, **2023**, *358*, 398–419. <DOI>.
- Nazha HM, Ammar B, Darwich MA, Assaad M, Response surface analysis of Zn–Ni coating parameters for corrosion

- resistance applications: a Plackett–Burman and Box – Behnken design of experiments approach, *Journal of Materials Science*, **2023**, 58(30), 12465–12480, <DOI>.
18. Obeyesekere N, Wylde J, Wickramarachchi T, Kemp L *et al.*, Formulation of Corrosion Inhibitors Using Design of Experiment (DOE) Methods and Discovering Highly Performing Inhibitors by High Throughput Experimentation (HTE) Methods Using Critical Micelle Concentration, NACE CORROSION; 2021, NACE, <DOI>.
 19. Akıncı S, Karaomerloğlu F, Kaygusuz E, A review on application areas and surface geometry in superhydrophobic materials, *Turkish Journal of Engineering*, **2024**, 8(1), 1–10, <DOI>.
 20. Mahbouli M, Identification d'inhibiteurs physiologiques de métallopeptidases impliquées dans la réponse nociceptive: Université Pierre et Marie Curie-Paris VI, 2015, <DOI>.
 21. Şenel M, Turhan Özdemir G, Optimization by response surface, 2021, <DOI>.
 22. Karabacakoğlu B, Tezaklı F, Electrocoagulation of corrugated box industrial effluents and optimization by response surface methodology, *Electrocatalysis*, **2023**, 14(2), 159–69, <DOI>.
 23. Gapsari Madhifitri F, Soenoko R, Suprpto A, Suprpto W, Minimization of corrosion rate using surface response methodology, *Engineering Review: Međunarodni časopis namijenjen publiciranju originalnih istraživanja s aspekta analize konstrukcija, materijala i novih tehnologija u području strojarstva, brodogradnje, temeljnih tehničkih znanosti, elektrotehnike, računarstva i građevinarstva*, **2018**, 38(1), 115–119, <DOI>.
 24. Hamidi F, Chaker H, Gil S, Cherif L, Saidi K, Vernoux P, Silver nanoparticles modified mesoporous titanosilicate materials for high oxidation of carbon monoxide, *Research on Chemical Intermediates*, **2021**, 47, 4443–4456, <DOI>.
 25. Chelilhi A, Hassaine R, Nachat S, Benabdallah M, Bendahou K, Aissaoui M *et al.*, One-pot green synthesis, study of fluorescence properties, and biological activity of pyrano [3, 2-c] chromenes derivatives via mesoporous materials MgO/SBA-15, *Journal of Heterocyclic Chemistry*, **2024**, 61(3), 439–457, <DOI>.
 26. Attar T, Benchadli A, Messaoudi B, Choukchou-Braham E, Corrosion inhibition efficiency, experimental and quantum chemical studies of neutral red dye for carbon steel in perchloric acidic media, *Chemistry & Chemical Technology*, **2022**, 16(3), 440–447, <DOI>.
 27. Attar T, Benchadli A, Choukchou-Braham E. Corrosion inhibition of carbon steel in perchloric acid by potassium iodide, *Inter. J. Adv. Chem.*, **2019**, 7, 35–41, <DOI>.
 28. Attar T, Benchadli A, Boulanour M, Choukchou-Braham E, Corrosion inhibition, adsorption and thermodynamic properties of poly (sodium 4-styrenesulfonate) on carbon steel in phosphoric acid medium, *French-Ukrainian Journal of Chemistry*, **2022**, 10(1), 70–83, <DOI>.
 29. Ebenso E, Alemu H, Umoren S, Obot I, Inhibition of mild steel corrosion in sulphuric acid using alizarin yellow GG dye and synergistic iodide additive, *International Journal of Electrochemical Science*, **2008**, 3(12), 1325–1339, <DOI>.
 30. Li X, Deng S, Fu H, Inhibition of the corrosion of steel in HCl, H₂SO₄ solutions by bamboo leaf extract, *Corrosion Science*, **2012**, 62, 163–175, <DOI>.
 31. Chabane N, Dergal F, Belarbi N, Chikhi I, Cherigui S *et al.*, Green inhibition of copper corrosion by ammoides verticillata oil in 1M nitric acid: weight loss and raman spectroscopic mapping studies, *Rev. Roum. Chim.*, **2023**, 68(7–8), 371–381, <DOI>.
 32. Attar T, Benchadli A, Choukchou-Braham E, Inhibition of corrosion of copper by polyvinylpyrrolidone-iodine in sulfuric acid medium, *Algerian Journal of Materials Chemistry*, **2022**, 5(1), 1–8, <DOI>.
 33. Yang X, Fu S, Wang Q, Sun Q, Zhang J, Peng Y *et al.*, Protective behaviour of naphthylamine derivatives for steel reinforcement in the simulated concrete pore solutions: Detailed experimental and computational explorations, *Journal of Molecular Structure*, **2022**, 1270, 133898, <DOI>.
 34. Verma C, Ebenso E, Quraishi MA, Ionic liquids as green and sustainable corrosion inhibitors for metals and alloys: An overview, *Journal of Molecular Liquids*, **2017**, 233, 403–414.
 35. Attar T, Benchadli A, Braham EC, Benkhaled A, Iodine– β -Cyclodextrin: An Effective Corrosion Inhibitor for Carbon Steel in Sulfuric Acid Solution-Experimental Design and Investigating Thermodynamic Parameters, *Journal of the Turkish Chemical Society Section A: Chemistry*, **2023**, 11(1), 161–170, <DOI>.
 36. Dehrı İ, Özcan M, The effect of temperature on the corrosion of mild steel in acidic media in the presence of some sulphur-containing organic compounds, *Materials Chemistry and Physics*, **2006**, 98(2–3), 316–323, <DOI>.
 37. T. Benabbouha, R. Nmila, M. Sinitı, K. Chefira, H. H. Rchid, *SN Appl. Sci.*, **2020**, 2, 662–669.
 38. Abd El Rehim S, Ibrahim MA, Khalid K, The inhibition of 4-(2'-amino-5'-methylphenylazo) antipyrine on corrosion of mild steel in HCl solution, *Materials Chemistry and Physics*, **2001**, 70(3), 268–273, <DOI>.
 39. Njoku CN, Onyelucheya OE, Response surface optimization of the inhibition efficiency of Gongronema latifolium as an inhibitor for aluminium corrosion in HCl solutions, *International Journal of Materials and Chemistry*, **2015**, 5(1), 4–13, <DOI>.
 40. Odejebi Oludare J, Akinbulumo Olatunde A, Modeling and optimization of the inhibition efficiency of Euphorbia heterophylla extracts based corrosion inhibitor of mild steel corrosion in HCL media using a response surface methodology, *Journal of Chemical Technology and Metallurgy*, **2019**, 54(1), 217–232, <DOI>.
 41. Olawale O, Bello J, Ogunsemi B, Uchella U, Oluyori A, Oladejo N, Optimization of chicken nail extracts as corrosion inhibitor on mild steel in 2M H₂SO₄, *Heliyon*, **2019**, 5(11), <DOI>.
 42. Azooz RE, EDTA as a corrosion inhibitor for Al in 0.5 M HCl: adsorption, thermodynamic and theoretical study, *Journal of Electrochemical Science and Engineering*, **2016**, 6(3), 235–251, <DOI>.